Journal of Chromatography A, xxx (2016) xxx–xxx

Contents lists available at ScienceDirect

Journal of Chromatography A

journal homepage: www.elsevier.com/locate/chroma

Molecular perspective of antibody aggregates and their adsorption on Protein A resin

Deqiang Yu[a,*], Yuanli Song[a], Richard Y.-C. Huang[b], Ryan K. Swanson[a], Zhijun Tan[a], Elizabeth Schutsky[a], Angela Lewandowski[a], Guodong Chen[b], Zheng Jian Li[a]

[a] Biologics Development, Global Manufacturing and Supply, Bristol-Myers Squibb Company, Devens, MA, USA
[b] Bioanalytical and Discovery Analytical Sciences, Research and Development, Bristol-Myers Squibb Company, Princeton, NJ, USA

ARTICLE INFO

Article history:
Received 4 April 2016
Received in revised form 9 June 2016
Accepted 9 June 2016
Available online xxx

Keywords:
Antibody aggregate
Protein A adsorption
Higher order structure
HDX-MS
Protein Conformational Array
Molecular modelling

ABSTRACT

Antibody aggregate is a common issue in therapeutic antibodies, which may compromise product efficacy and cause adverse effects. Antibody aggregate level is normally controlled in bioprocessing by polishing steps after Protein A capture. This paper studied the Higher Order Structures (HOS) of antibody aggregates (dimer H1 and H2) and their adsorption on Protein A resin and thus elucidated the mechanism using Protein A capture for enhanced aggregate removal. The HOS of antibody aggregates and their complex with Protein A were characterized using HDX-MS combined with SEC-MALS, Protein Conformational Array (PCA), and molecular modeling. The aggregate size and Protein A binding ratio suggested that H2 has much more compact structure than H1. HDX-MS and PCA further revealed that H1 was formed by single Fab-Fab interaction while H2 formed by Fab-Fab and likely Fc-Fc interaction. On Protein A resin, both the molar binding ratio and the correlation between protein size and ligand distance support that each monomer can only bind one Protein A ligand, while each dimer can bind two ligands, thus resulting in stronger resin binding. Furthermore, dimer H2 binds stronger than dimer H1 due to its compact structure. By integrating biophysical analysis and molecular modeling with process development, this study revealed the antibody aggregate structures and the mechanism of aggregate removal using Protein A chromatography. It also provided a general strategy for in-depth product and process understanding in antibody and other biologics development.

1. Introduction

Understanding a biopharmaceutical product and process at the molecular level can help the design of a more efficient process and support the correlation of critical quality attributes with clinical performance. This paper studies the HOS of antibody aggregates and their adsorption on Protein A resin, which leads to in-depth understanding of antibody aggregates and their removal by Protein A chromatography.

Protein A chromatography is critical for platform-based antibody purification. Due to the specific adsorption of antibodies, it is widely used for antibody capture from harvest and removal of process-related impurities including HCP, DNA and viruses [1–3]. However, it is rarely used for removal of an important class of product-related impurities, antibody aggregates from harvest, due to lack of understanding of aggregates and their interaction with Protein A.

Antibody aggregate is a common issue in antibody therapeutics [4]. Antibody aggregate poses the risks of compromised product efficacy due to different biological activity from monomer, and generation of adverse effects such as immune response caused by neutralizing antibodies [5–8]. Therefore, antibody aggregate needs to be removed to a low level in antibody purification. However, this is more difficult than removal of process related impurities due to the biophysical similarities between the aggregate and monomer, the multiple sources and types of aggregate, and less understanding of aggregation mechanism. From the bioprocessing point of view, antibody aggregates could be formed during cell culture expression and downstream purification. Due to the different unit-operations and process conditions, the aggregates could be soluble/insoluble, covalent/non-covalent, and reversible/irreversible. In antibody processing, aggregate removal generally relies on polishing steps after Protein A capture. However, the aggregate removal capability of polishing steps is limited for both total aggregates and specific

* Corresponding author.
E-mail addresses: deqiang.yu@bms.com, dennis.yudeqiang@gmail.com (D. Yu).

http://dx.doi.org/10.1016/j.chroma.2016.06.031
0021-9673/

species. Furthermore, the trend of using only one polishing step increases difficulties in aggregate removal.

Cell culture harvest usually contains the highest level of aggregate in the process. If aggregate level can be reduced in the Protein A step, it will significantly improve the overall process robustness for aggregate removal. Separation of antibody aggregate by Protein A chromatography was explored in a few reports [9,10]. One report demonstrated aggregate removal by linear pH-gradient using POROS Protein A for a few hIgG1 and hIgG2 [9]. Another one used similar strategy to remove antibody aggregate and other impurities with different resins [10]. However, none of these reports studied the mechanism of aggregate removal using Protein A chromatography. To utilize Protein A for aggregate removal in a process, it is important to understand the structures of aggregates and how they interact with Protein A resin, which is the focus of this study.

HOS determination is challenging for large proteins like antibodies. It is even more challenging for antibody aggregates due to their formation through multiple possible interactions between monomers. Therefore, structure determination of antibody aggregate requires a variety of orthogonal biophysical tools to make a complete picture. Multi-Angle Light Scattering (MALS), Dynamic Light Scattering (DLS) and analytical ultracentrifugation are used to determine protein size and molecular weight [11–14]. Differential Scanning Calorimetry and Circular Dichroism are traditionally used to monitor stability and protein structure changes [15–17]. These traditional methods only provide global changes in HOS with low resolution. X-ray Crystallography and Nuclear Magnetic Resonance can provide high resolution structural information but they are very time-consuming or not suitable for large proteins like antibodies, aggregates, or complexes [18,19]. Hinge region flexibility also makes antibody crystallization very difficult. MS, on the other hand, has been widely used to characterize protein sequence and structure for large glycosylated proteins such as antibodies [13]. Hydrogen/Deuterium Exchange Mass Spectrometry (HDX-MS), a unique MS-based protein footprinting strategy, has been used to determine protein conformation and conformational dynamics by monitoring the hydrogen-deuterium exchange rates. The level of HDX depends on the solvent accessibility of backbone amide hydrogen atoms and the protein hydrogen bonds [20–23]. HDX-MS has successfully revealed the protein interface in reversible antibody self-association, and in a structural investigation of site-specific antibody drug conjugate [19,24]. Protein Conformational Array is a new and complementary technique to determine protein HOS. This ELISA-based method can detect the epitopes on an antibody using a panel of 34 antibodies raised against peptides derived from the full length protein sequence of eight commercial monoclonal antibody drugs [25,26]. It is relatively straightforward to perform the analysis. Recently, the IgG1 mAb high order structures, specifically dimers, were studied using Transmission Electron Microscopy and hydroxyl radical footprinting but the interface information was not discovered [27,28].

Molecular modeling and simulation are useful tools to construct protein structures and design new proteins [29]. They are especially useful for the characterization of antibodies, antibody aggregates, and complexes because obtaining the full-length structures of these large proteins at the atomic-level is difficult if solely based on experimental approaches. Crystallohydrodynamics modeling was used to determine IgG domain orientation and solution conformation [30,31]. Using molecular dynamics simulation, an all-atom model for trastuzumab was established for representative structure in aqueous solution from the crystal structures of antibody fragments [18]. More recently, homology modeling was used to design and select therapeutic antibody candidates using developability index, an aggregation propensity indicator combining hydrophobic and electrostatic interaction [32,33].

In this study, antibody aggregates demonstrated stronger binding than monomer on Protein A resin while two types of aggregates also bound differently. To understand the aggregates and their adsorption on Protein A resin, the monomer and aggregates were purified and characterized by a set of biophysical tools for structural information and also reacted with Protein A ligand to determine the binding ratio. MALS was used to determine the sizes and molecular weights of aggregates and antibody-Protein A complexes. The protein interfaces in aggregates were characterized by HDX-MS and PCA. Molecular modeling and simulation synergized the structural information from different angles to predict the three-dimensional (3D) structures for monomer, aggregates and antibody-Protein A complexes. The structural information combining with quantitation of Protein A binding on resin was then used to elucidate aggregate adsorption on Protein A resin. Our finding reveals the aggregate structures and the mechanism of aggregate removal using Protein A chromatography for in depth product and process understanding.

2. Experimental

2.1. Preparation of monomer, aggregates and their complex with Protein A

Superdex 200 Increase 10/300 GL column (GE Healthcare) was used to prepare monomer and aggregates from Protein A purified antibody (Supplementary Experimental). 0.5 mL Protein A purified mAb (20 mg/ml) was loaded to the column and eluted using 200 mM potassium phosphate, 150 mM NaCl, pH 6.8 buffer (PBS). The elution was collected with 0.5 mL fractions. The aggregate and monomer peaks were pooled separately based on the order of elution and named H1 for HMW Species 1, H2 for HMW Species 2, and M for monomer. Multiple runs were performed to increase the amount of aggregates. Purified monomer, H1 and H2 were mixed respectively with Protein A ligand for MabSelect SuRe (Repligen) with a monomer: Protein A molar ratio of 1:1.1 for monomer and 1:1.4 for H1 and H2. The mixture was incubated at room temperature for half an hour and the samples were then analyzed by SEC-MALS.

2.2. SEC-MALS and DLS

The antibody species and their complex with Protein A were analyzed by SEC using a tandem column of TSKgel G 3000SWxl (TOSOH Bioscience) on Waters HPLC e2695 Alliance. The mobile phase of PBS was applied at a flow rate of 0.5 mL/min. The signals of UV, light scattering and refractive index were respectively monitored by 2489 UV/Vis detector (Wyatt), miniDAWN TREOS (Wyatt) and Optilab T-rEX (Wyatt). The data was processed by ASTRA 6.1(Wyatt). The antibody species in PBS were analyzed at 25 °C for hydrodynamic diameter (D_h) in disposable folded capillary cell (DTS1070) using Zetasizer Nano ZSP (Malvern Instruments).

2.3. Protein Conformational Array

PCA was performed to study the 3-D conformational difference between monomer and aggregates using InnoBridge ELISA kit (ArrayBridge) following vender's instruction. Briefly, the ELISA plate was coated with incubating 100 μL of 5 μg/mL monomer or aggregates solution for 1 h. After washing away unbound monomer or aggregates, 100 μL biotin-conjugated capture antibody was added and incubated for 1 h. After washing away unbound capture antibody, Horse Radish Peroxidase (HRP)-conjugated streptavidin was added and incubated for 45 min to bind to biotin-conjugated antibody. After washing, TMB substrate was added and converted

Please cite this article in press as: D. Yu, et al., Molecular perspective of antibody aggregates and their adsorption on Protein A resin, J. Chromatogr. A (2016), http://dx.doi.org/10.1016/j.chroma.2016.06.031

by the captured HRP to a colored product. After a 15-min incubation for color developing, the reaction was stopped by adding acidic stop solution and the intensity of the generated yellow color was detected at 450 nm wavelength in a microtiter plate reader. Each antibody species was carried out in duplicate. The histogram representing signals from 34 antibodies was achieved for monomer and aggregates.

2.4. HDX-Mass Spectrometry

HDX differential studies of purified mAb C monomer, H1 and H2 were conducted using continuous labeling approach. HDX was initiated by diluting 5 μL of the protein stock solution into 55 μL of D2O buffer (10 mM phosphate in D2O, pD 7.0). After continuous labeling for 20 s, 1 min, 10 min and 4 h at 4 °C, the exchange reaction was quenched by adding quenching buffer (100 mM phosphate buffer with 4 M GdnCl and 0.4 M TCEP, pH 2.5, 1:1, v/v). 50 μL of the quenched solution was then injected into a Waters HDX system. Proteins were digested inline using an immobilized pepsin column (Waters, 2.1 × 30 mm) at 20 °C for 3 min. The resulting peptides solution was desalted with a Waters VanGuard C18 trapping column (2.1 × 5 mm). Peptides were then separated in a reverse-phase column (Waters BEH C18 column, 1.0 × 50 mm) with a 9 min LC gradient. The gradient settings were: 8–40% solvent B for 6 min, isocratic flow at 40% solvent B for 1 min, 40–85% solvent B for 0.5 min, isocratic flow at 85% solvent B for 1 min, and then a return to 8% solvent B for 0.5 min. Solvent A was water containing 0.1% formic acid, and solvent B was acetonitrile containing 0.1% formic acid. Peptide capture and separation were carried out at 0 °C, and the peptide analysis was conducted on a Synapt G2-Si mass spectrometer running in the ESI positive mode with ion-mobility switched on. The instrument parameters were set as following: ESI voltage 3.5 kV, cone voltage 35 V, source temperature 80 °C, desolvation gas- nitrogen at 175 °C and 600 L/h, IM Triwave velocity at 650 m/s and wave height at 40 V. Each experiment was carried out in duplicate.

Prior to HDX experiments, non-deuterated experiments were conducted and acquired with MSE fragmentation to generate a list of common peptides for mAb C. The MS/MS data were analyzed using Waters ProteinLynx Global Server, providing 88% sequence coverage for heavy chain, and 97% sequence coverage for light chain. HDX data were analyzed by Waters DynamX software to generate differential HDX plots.

2.5. Binding capacity test of antibody species on Protein A resin

96-well plate format of Protein A resin was used to test binding capacity for monomer, H1 and H2. 40 μL of 10% well-mixed MabSelect SuRe resin suspension was loaded into plate wells. Monomer was first used to test the impact of incubation time (1, 4 and 20 h) on binding capacity at representative 35 mg/ml resin loading. Purified monomer, H1 and H2 were then respectively added into the plate wells at duplicate with 35 mg/mL resin loading and incubated with the resin for chosen 4 h at 900 rpm shaker speed. After incubation, the resin was settled down by centrifuge and the supernatant was tested by UV280 to determine remaining protein concentration. The binding capacity of each antibody species on Protein A resin was then determined by (Loading amount – Remaining amount)/Resin volume.

2.6. Molecular modeling and simulation

Homology model of mAb C were generated using the Discovery Studio software package (Accelrys Inc.). Full length antibody structures, 1IGY and 1IGT [34,35] were selected as templates for homology modeling, as they have over 80% sequence identity to mAb C, and most sequence differences are restricted to the CDR region. Sequence alignments were optimized and 3D homology models built using MODELER [36]. The homology models were submitted to side chain optimization and energy minimization steps, followed by model validation.

Possible H1 and H2 dimers were first generated with Chimera [37] according to the predicted structures by gyration radius and Protein A binding ratio and then confirmed by PCA results and the interfaces provided by HDX-MS experiments. The dimers underwent energy minimization using GROMACS [38] force field to remove unrealistic side chain contacts.

The homology model of Protein A was generated with Chimera using the structure of Protein A Z domain (2SPZ) [39] as a template. The complexes of antibody and Protein A were generated using the pdb file of Fc and Protein A complex (1L6X) [40] as a template. The gyration radius of monomer, dimers, and their complexes with Protein A were calculated using Pymol (V1.7.4 Schrödinger LLC).

3. Results and discussion

3.1. HMW binding on Protein A resin and SEC-MALS analysis

During mAb process development, we found in different antibodies including hIgG1 and hIgG4, Protein A elution pH has a significant impact on aggregate level in elution pool. To understand the impact, pH gradient was used for antibody elution to profile the distribution of aggregates. For mAb C, an hIgG4 focused in this study, Protein A elution pool was found by SEC-MALS analysis to contain two major species of HMW named as H1 and H2 (Fig. 1A). The MW of monomer is 148.7 ± 0.4 kDa, very close to the theoretical 146.5 kDa. The MW of H1 is 304.4 ± 4.3 kDa and the MW of H2 is 280.3 ± 11.7 kDa. Both MWs of H1 and H2 are close to the theoretical 293.0 kDa for dimer. However, the gyration radius of H1 (8.8 ± 0.6 nm) is much bigger than H2 (5.9 ± 1.4 nm) while H2 is only slightly bigger than monomer (5.0 ± 1.1 nm). Fig. 1C and 1D show the HMW and monomer composition in each gradient fraction. Monomer eluted earlier, while HMW eluted later. The elution of Monomer, H1 and H2 started from eluate fraction pH 5.0, 4.6 and 4.2 respectively, which clearly demonstrated stronger binding of HMW than monomer, and stronger binding of H2 than H1. To prove that the aggregate in elution originated from harvest, the mass balance of aggregate in the load and elution pool was analyzed by SEC-HPLC. H1 was fully recovered at 102% in the elution, while 74% of H2 was recovered in the elution, with the remaining H2 presumably still bound to the column due to its stronger binding than H1. No increase of H1 and H2 and no other aggregate species were observed in elution. Furthermore, the stability study (Fig. 1B) showed mAb C only started to aggregate at pH < 3.4 while the fraction pH ranged from 3.6 to 5.0. Both experiments demonstrates that the aggregate originated from the harvest instead of formation by low pH.

3.2. Preparation, MALS analysis and molecular modeling of HMW and their Protein A complexes

To study HMW structures, monomer, H1 and H2 were purified from Protein A elution pool using semi-preparative SEC. The purity of monomer, H1 and H2 are 99.6%, 91.6% and 81.9% respectively by SEC-MALS (Fig. 2). Protein A ligand stock was found to have 53% of dimer and only 43% of monomer by SEC-MALS. Protein A ligand for MabSelect SuRe contains a cysteine residue for immobilization on resin [41,42], which could cause ligand dimerization in solution. The Protein A ligand was reduced by DTT and alkylated by iodoacetamide to increase Protein A monomer to 77.3% by SEC-MALS. The molecular weight of Protein A monomer was found

Please cite this article in press as: D. Yu, et al., Molecular perspective of antibody aggregates and their adsorption on Protein A resin, J. Chromatogr. A (2016), http://dx.doi.org/10.1016/j.chroma.2016.06.031

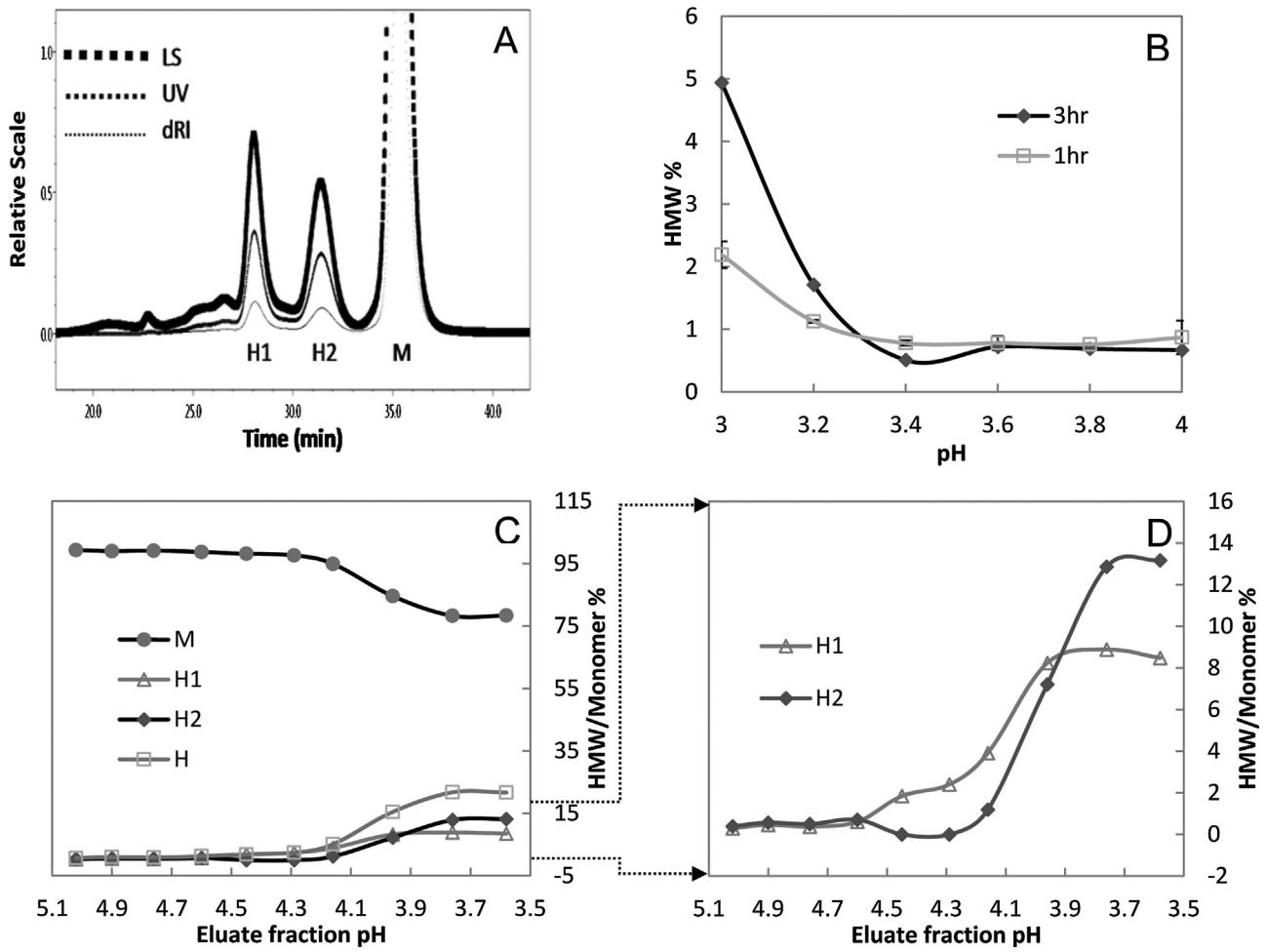

Fig. 1. Analysis of Protein A eluate fractions using SEC-MALS. (A) SEC-MALS analysis of Protein A eluate fractions; (B) HMW level of mAb C in pH stability study; (C) Correlation of monomer and HMW level with eluate fraction pH, and (D) Enlarged figure for H1 and H2. M, monomer; H, HMW; H1 and H2, two dimer species; LS, light scattering; dRI, differential refractive index.

Table 1
Comparison of MW and Gyration radius by MALS with predicted values.

	MW by MALS (kDa)	MW Predicted (kDa)	Rg by MALS (nm)	Rg Predicted[c] (nm)
A	27.6 ± 1.1	26.7[a]	/	/
M	150.5 ± 1.6	146.5[a]	5.0 ± 0.3	5.3
H1	310.3 ± 10.4	293.0[a]	8.7 ± 0.7	8.0
H2	290.2 ± 10.8	293.0[a]	5.6 ± 0.2	5.8
MA	179.8 ± 1.6	178.1[b]	6.2 ± 0.2	6.5
$H1A_4$	467.6 ± 32.5	420.7[b]	11.5 ± 1.6	9.9
$H2A_3$	372.3	373.0[b]	NT	7.8

Notes: (Mean value ± Standard error) from three samples. NT: Not tested.
A, Protein A; M, monomer; H1 and H2, two dimer species; MA, monomer-Protein A complex at 1:1 molar ratio; $H1A_4$, H1-Protein A complex at 1:4 molar ratio; $H2A_3$, H2-Protein A complex at 1:3 molar ratio.
[a] Theoretical MW from amino acid sequence.
[b] Calculated MW from the MW of reactants by MALS.
[c] Predicted by molecular modeling.

to be 27.6 ± 1.1 kDa, which matches well the theoretical 26.7 kDa [41–43].

Since monomer, H1 and H2 bind to Protein A resin at different strength, antibody-Protein A complexes were prepared to study the Protein A binding ratios. The complex peaks were identified by molecular weight and gyration radius from MALS analysis. As shown in Fig. 2, monomer-Protein A complex with 1:1.1 molar ratio demonstrated complex peaks with all monomer and Protein A consumed. The complex at 33.0 min is MA composed of one monomer and one Protein A (179.8 kDa by MALS vs 178.1 kDa by calculation). The monomer binding two Protein A ligands (AMA) is easy to grow into bigger complexes, one of which is $A(MA)_3$ at retention time of 26.1 min (583.4 kDa by MALS vs 561.9 kDa by calculation). The H1-Protein A complex (1:1.4 monomer-Protein A molar ratio) demonstrated an apparent species at 26.5 min, $H1A_4$ composed of one H1 dimer and four Protein A (467.6 kDa by MALS vs 420.7 kDa by calculation). The big size of H1 might enhance the collision with Protein A ligands with some bigger complexes observed. The H2-Protein A complex (1:1.4 monomer-Protein A molar ratio) contained a major species at 28.8 min, $H2A_3$ composed of one H2 dimer

Please cite this article in press as: D. Yu, et al., Molecular perspective of antibody aggregates and their adsorption on Protein A resin, J. Chromatogr. A (2016), http://dx.doi.org/10.1016/j.chroma.2016.06.031

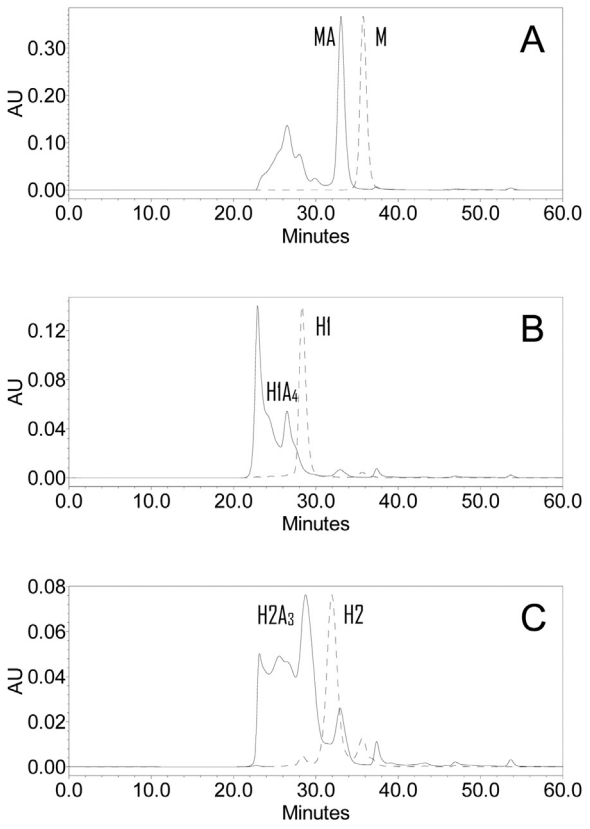

Fig. 2. SEC-MALS analysis of antibody-Protein A complex (solid line) overlapped with the antibody reactant (dotted line). (A) Monomer-Protein A complex overlapped with monomer; (B) H1-Protein A complex overlapped with H1; (C) H2-Protein A complex overlapped with H2.

and three Protein A (372.3 kDa by MALS vs 373.0 kDa by calculation). Very likely the compact structure of H2 caused the steric hindrance of one Protein A binding site. As summarized in Table 1, the experimental molecular weight and gyration radius of major complexes were compared with calculated molecular weight from reactants and predicted gyration radius from molecular modelling (Fig. S1). For MA, the MW and radius by MALS matches the predicted ones very well. For $H1A_4$, both MW and radius by MALS are slightly bigger than predicted ones, probably due to the structure flexibility of four long Protein A ligands in solution. For $H2A_3$, the MW by MALS matches the predicted one very well.

The SEC-MALS analysis of monomer, dimers and their complex with Protein A provided a big picture for the distinctive structures of two dimers based on molecular weight, protein size, and Protein A binding ratio. The apparently bigger size of dimer H1 than H2 indicates an extended structure for H1 but a very compact one for H2. Furthermore, H1 binding up to four Protein A ligands in solution indicates all four Protein A binding sites from two monomers are fully exposed, while H2 binding three Protein A ligands indicates the steric hindrance for one Protein A binding site. Based on above information, molecular modeling was used to predict H1 and H2 structures (Fig. S1). H1 structure with one Fab-Fab interaction (Fig. S1B) is fully extended and matches well the gyration radius and four potential Protein A binding sites. H2 structure has two options matching the compact size. One has cross-linked four Fabs with upper hinge region interaction (Fig. S1C), which may bind up to four Protein A ligands. Another structure (Fig. S1D) based on Fab-Fab and Fc-Fc interactions could bind potentially three Protein A ligands due to the steric limitation in the cavity between two monomers. Both H2 structures match the compact protein size but the structural model with Fab-Fab and Fc-Fc interactions is more supported by the 1:3 Protein A binding ratio.

3.3. HMW interface characterization by HDX-MS and PCA

HDX-MS and PCA were used to reveal the monomer interfaces in dimers. PCA as a simple tool was used to provide preliminary information for structure change between monomer and dimers. As shown in Fig. 3, similar signals were detected between the monomer and two dimers for most of the 34 epitopes examined. The systematic slightly higher signal in monomer is likely caused by the normalization of molar amount. The apparent signal differences between the monomer control and dimers are observed on Ab 6, 15, 17 and 20. Ab 6 represents the epitope on LC variable region (Light Chain, CDR3), Ab 15 and 17 the LC constant region, and Ab 20 the end of HC constant region 1 (Heavy Chain). The epitopes on LC represented by Ab 6, 15, and 17 have significantly increased exposure in H1 and slightly increased exposure in H2. The conformational changes across variable and constant regions on LC indicates that dimer formation might occur through the Fab domain. Furthermore, the interactions on H1 Fab are stronger than those on H2 Fab. The exposure of Ab 20 epitope in H2 but not in H1 further indicates the different dimer interface between H1 and H2.

HDX-MS was used to elucidate the interaction details at molecular level. Peptide regions that display more deuterium uptake in monomer indicate HDX reductions upon the formation of dimers due to protein self-association. This pinpoints the potential protein aggregation interfaces. In HDX analysis of M and H1 (Fig. 4), significant HDX reductions (>3x STD) were observed in five peptide regions (residues 27–32, 54–58, 69–79, 123–140 and 202–205) in the Fab domain of heavy chain from H1. Peptide region 196–214 in light chain also exhibited significant HDX reduction. Interestingly, two peptide regions (residues 33–49 and 162–175) in light chain showed more deuterium uptake, suggesting protein self-association-induced conformational changes.

In HDX analysis of M and H2 (Fig. 5), unlike H1, the levels of HDX reduction observed in H2 were relatively low. However, two peptide regions (residues 27–32 and 54–58) in heavy chain CDRs, that showed significant HDX reductions in H1, also displayed significant HDX reductions in H2, indicating their importance in protein-protein self-association. Interestingly, peptide region 33–49 in light chain also showed reversed trend of HDX upon H2 formation. This suggests that the conformational change of peptide region 33–49 in light chain was mostly induced by the protein-protein interactions in residues 27–32 and 54–58 in heavy chain CDRs.

To correlate the HDX results with the structures of H1 and H2, the peptides showing significant HDX reduction (red and orange) or reversed trend (green) were mapped onto an in-house crystal structure of Fab (Fig. 6). As expected for H1 (Fig. 6A), peptides that showed significant HDX reductions are all located in the same interface of Fab, including part of the CDRs, and are mostly comprised of β sheet-loop-β sheet structure. The residues 27–32 and 54–58 combined with residue 69–79 on HC are one of the key protection sites on top of Fab (Site 1). They form a compact 3D region which facilitates their interaction. Due to the Site 1 interaction on HC, the corresponding residues 33–49 on LC are more exposed. On the lower part of Fab, residues 123–140 and 202–205 on HC and 196–214 on LC forms another key interaction site (Site 2). Correspondingly, this interaction site caused the exposure of residues 162–175 on LC, which matches well with Ab 15 exposure (residues 152–175 on LC) by PCA. HDX results clearly yield good correlation with the predicted structural model of Fab-Fab interactions in H1 (Fig. S1B).

The low levels of HDX reduction observed in H2 suggest that the protein-protein associations in H2 mainly involve protein side chain-side chain interactions on the top of Fab, which have limited

Please cite this article in press as: D. Yu, et al., Molecular perspective of antibody aggregates and their adsorption on Protein A resin, J. Chromatogr. A (2016), http://dx.doi.org/10.1016/j.chroma.2016.06.031

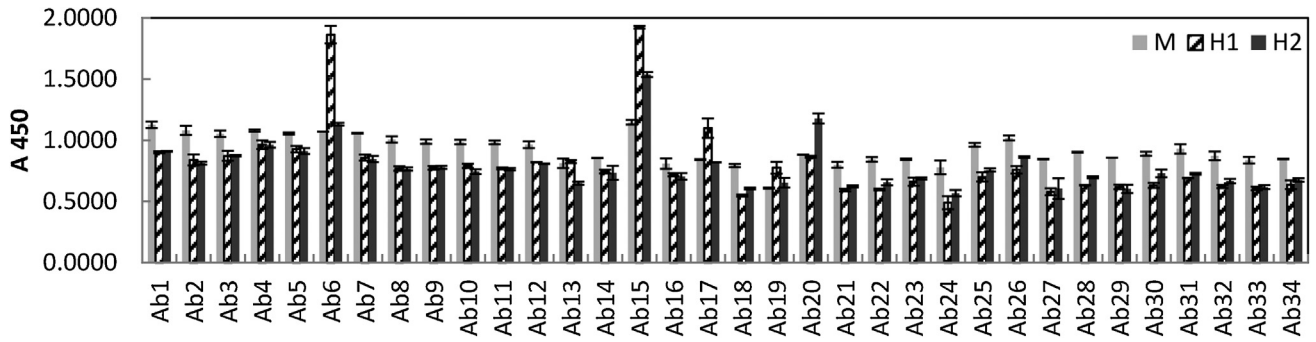

Fig. 3. Protein Array analysis of M, H1 and H2. Samples were run on duplicate using InnoBridge ELISA kit. A panel of 34 Abs targeting antibody epitopes was used to probe the structure difference between monomer, dimer H1 and H2.

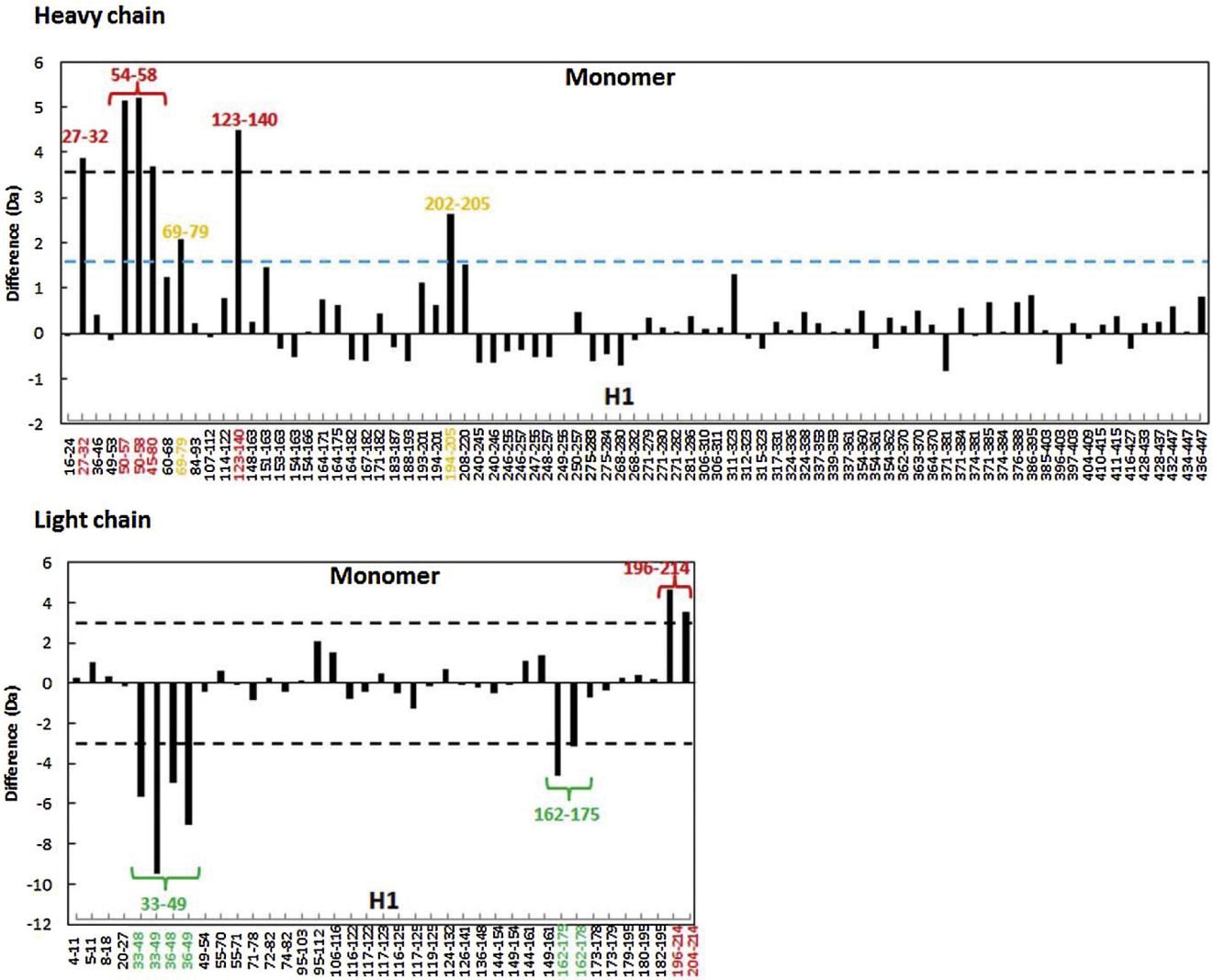

Fig. 4. Differential HDX of heavy chain (top) and light chain (bottom) of M and H1 ($\Delta D = D$ uptake of M–D uptake of H1). ΔD of common peptides from M and H1 for four exchange time points were summed (black bar). Peptides with HDX reduction ≥ 3.5 D were colored in red, and those in the range of 1.5–3.5 D were colored in orange. Peptides that showed reversed trend of HDX were colored in green. (For interpretation of the references to colour in this figure legend, the reader is referred to the web version of this article.)

impact on the solvent accessibility of protein amide backbone. As shown in Fig. 6B, during H2 formation there is similar protection on the top of Fab composed of residues 27–32 and 54–58 but no protection on the lower part of Fab. This interaction site caused the exposure of residues 33–49 on LC. Although HDX results do not show direct evidence for Fc-Fc interactions in the predicted structural model of H2 (Fig. S1D), detailed molecular-level information of potential protein aggregation interfaces on the top of Fab are revealed by HDX experiments. Therefore, the structural model with upper Fab-Fab and lower Fc-Fc interaction (Fig. S1D) is more supported than the model with strong interaction at hinge region (Fig. S1C). Furthermore, although not a strong signal from

Please cite this article in press as: D. Yu, et al., Molecular perspective of antibody aggregates and their adsorption on Protein A resin, J. Chromatogr. A (2016), http://dx.doi.org/10.1016/j.chroma.2016.06.031

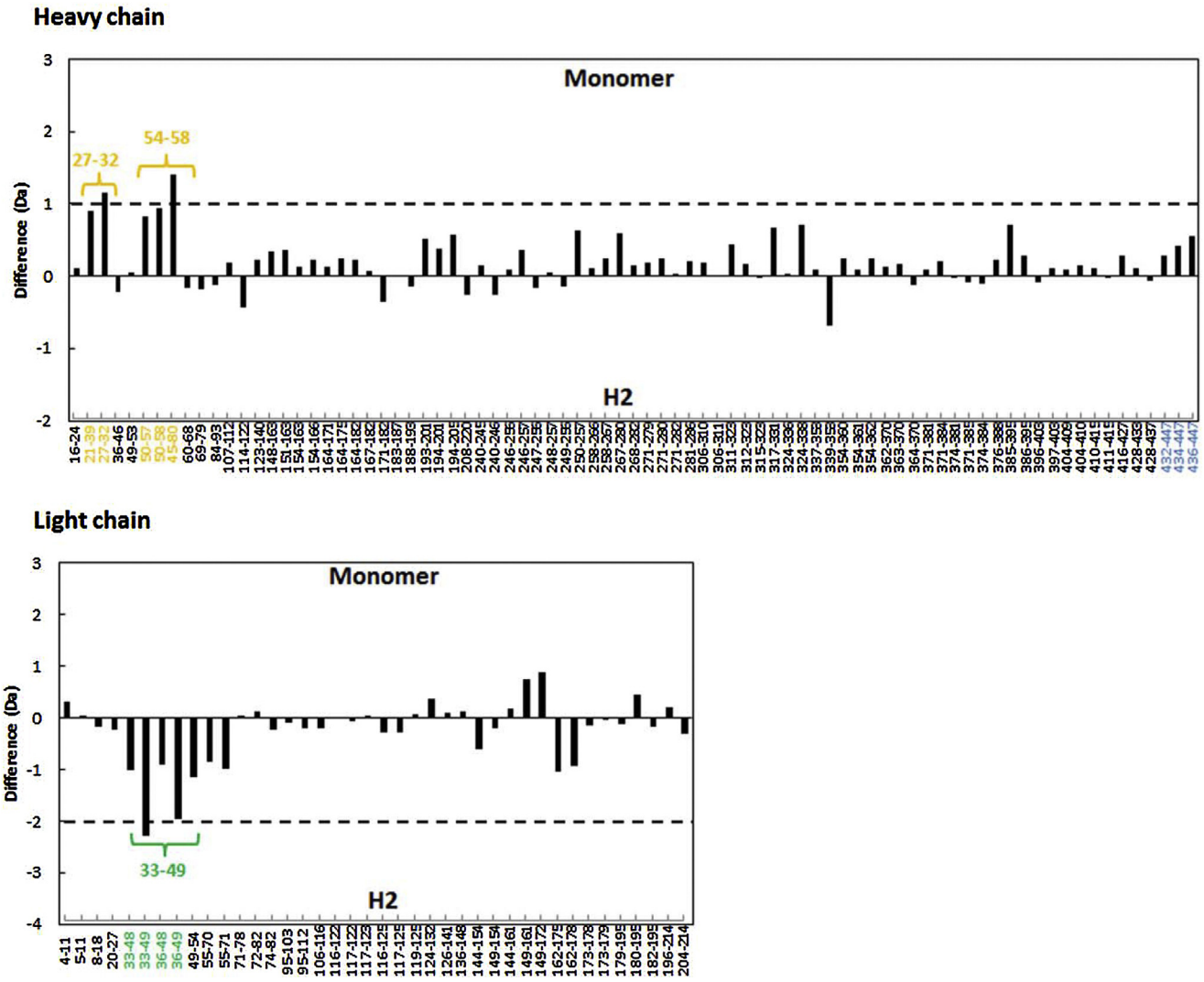

Fig. 5. Differential HDX of heavy chain (top) and light chain (bottom) of M and H2 (ΔD = D uptake of M–D uptake of H2). ΔD of common peptides from M and H2 for four exchange time points were summed (black bar). Peptides with HDX reduction ≥1 D were colored in orange. Peptides that showed reversed trend of HDX were colored in green.

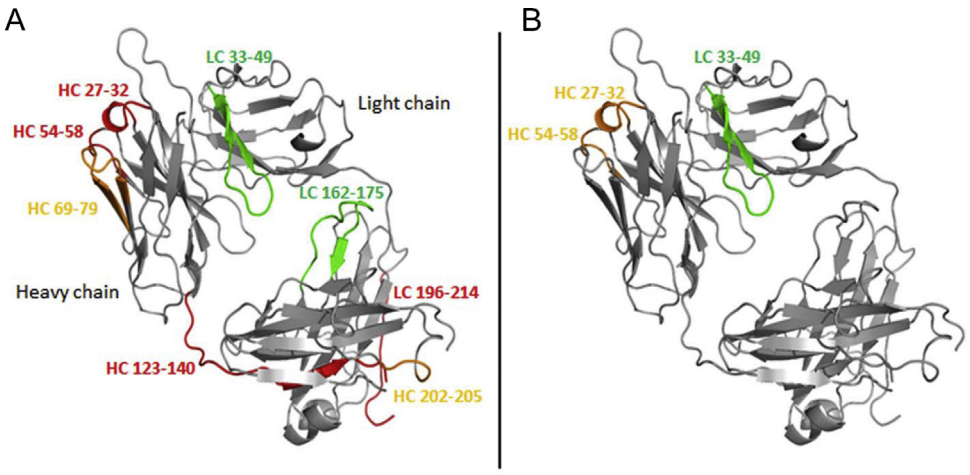

Fig. 6. Differential HDX mapping on mAb C Fab crystal structure. (A) M vs. H1; (B) M vs. H2. For H1, peptides with HDX reduction ≥3.5 D were colored in red, and those in the range of 1.5–3.5 D were colored in orange. For H2, peptides with HDX reduction ≥1 D were colored in orange. Peptides that showed reversed trend of HDX were colored in green. (For interpretation of the references to colour in this figure legend, the reader is referred to the web version of this article.)

Please cite this article in press as: D. Yu, et al., Molecular perspective of antibody aggregates and their adsorption on Protein A resin, J. Chromatogr. A (2016), http://dx.doi.org/10.1016/j.chroma.2016.06.031

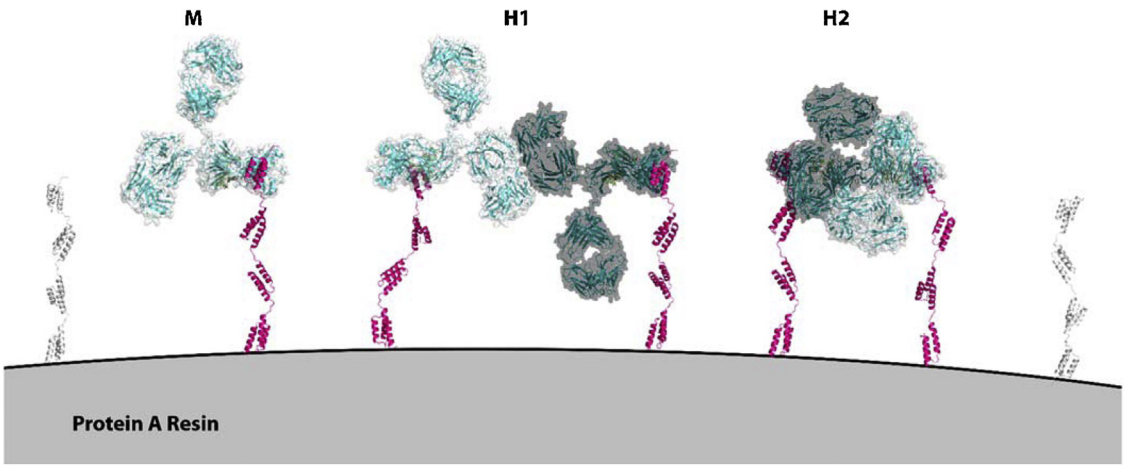

Fig. 7. Interaction of different mAb species (M, H1, and H2) with protein A on resin. Protein A ligands composed of four tandem triple helical bundle Z-domains are immobilized on the resin surface. mAb species (M, H1, and H2) bind to the resin via the interaction between the Protein A binding sites and Protein A Z domains. The Protein A ligands engaged in binding are shown in red and free Protein A in gray. (For interpretation of the references to colour in this figure legend, the reader is referred to the web version of this article.)

HDX-MS results, there is an increasing reduction signal on residues 436–447 indicating potential weak interaction at the end of Fc (Figs. 5 and Fig.S2B). This Fab-Fab and Fc-Fc model correlates well with the compact structure of H2 and the 1:3 Protein A binding ratio.

Combining HDX with PCA and molecular modeling data, dimer H1 is most likely formed by the interaction of Fab Site 1 on one monomer with Fab Site 2 on the other (Figs. 6 A, Fig. S1B and Fig. S2A). H2 is most likely formed by symmetrical interaction between the top of Fabs from both monomers with weak interaction at the end of Fc (Figs. 6 B, Fig. S1D and Fig. S2B). Therefore, the structural information from combined biophysical tools was integrated with molecular modeling and provided a complete picture of H1 and H2.

3.4. Interaction of antibody species with Protein A on resin

The above structure information of monomer and HMW provides insights into their binding and elution behavior on Protein A resin. Fig. 7 depicts the most possible interaction model of monomer and dimers on Protein A resin. IgG monomer, although with two Protein A binding sites, can only interact with one Protein A ligand on resin. The dimer H1 can bind up to four free Protein A ligands in solution but only interact with two on the resin due to the steric hindrance. For the same reason, the dimer H2 also interacts with two ligands on the resin, less than three it can bind in solution.

To quantitatively determine Protein A binding ratio on resin, binding capacity of Monomer, H1 and H2 was tested using batch mode adsorption. The loading of 35 mg/mL was the same as the column mode and representative in processing. Four hours incubation was chosen since incubation study using monomer demonstrated highest binding at 4 h (30.7 ± 0.7, 33.3 ± 0.3 and 29.2 ± 1.9 mg/ml for 1, 4 and 20 h respectively). Slightly lower binding at 20 h might be caused by protein degradation and method variation. Using batch mode adsorption on the same plate, the binding capacity of monomer, H1 and H2 was determined to be 31.5, 32.1 and 31.5 mg/mL respectively (Table 2). With Protein A ligand density of 5.7 mg/mL (average of 5.6, 5.6 and 5.9 mg/mL from 3 lots) [42] and the molecular weights of Protein A and antibody species by MALS (Table 1), the Protein A: Antibody species molar ratio was determined to be 1.0, 2.0, and 1.9 for Monomer, H1 and H2 respectively (Table 2). The binding ratio demonstrates that on average, one monomer interacts with one Protein A ligand while both H1 and H2 interact with two Protein A ligands on the resin, which correlated well with the model (Fig. 7).

Table 2
Protein A binding ratio on resin per antibody species and their hydrodynamic diameters.

Antibody species	M	H1	H2
Binding capacity (mg/ml resin)[a]	31.5 ± 0.1	32.1 ± 0.1	31.5 ± 0.0
Protein A to Antibody species molar ratio[a]	1.0 ± 0.005	2.0 ± 0.009	1.9 ± 0.000
Hydrodynamic diameter (nm)[b]	12.6 ± 0.1	20.4 ± 0.3	21.1 ± 0.6

Notes: (Mean value ± Standard error) from two samples (a) and three samples (b).

The Protein A binding ratios for monomer, H1 and H2 are further supported by correlating the hydrodynamic diameters of monomer, H1 and H2 with the Protein A ligand distribution on the resin. The average distance between two adjacent Protein A ligands is calculated as 19.7 nm based on the surface area of 50 m^2/mL and ligand density of MabSelect SuRe resin [42,44] (Supplementary Results). The D_h of monomer, H1 and H2 are 12.6, 20.4 and 21.1 nm respectively (Table 2). D_h indicates the apparent size of the dynamic hydrated molecules, which includes both hydration and shape information. Previously gyration radius was used for structure analysis because it indicates molecular shape information. Although H1 and H2 have different Rg reflecting different structure, their similar D_h suggests similar diffusion behavior on resin surface when interacting with Protein A ligands. Monomer has two Protein A binding sites on the same Fc and thus can only bind one Protein A ligand. However, due to the bigger D_h of H1 and H2 than the ligand distance and the spread of Protein A binding sites on both end of the dimers (Fig. S1B and S1D), the dimers most likely bind two adjacent Protein A ligands whose flexibility can also contribute to the interaction. Due to the diffusion limitation, the accessible surface area for Protein A ligand should be smaller than the total 50 m^2/mL and thus, the actual ligand distance is shorter than 19.7 nm. This will make H1 and H2 more accessible to interact with two adjacent Protein A ligands.

Both Protein A binding ratio on resin and the size correlation between antibody species and ligand distance support the interaction of both dimers with two Protein A ligands on resin. Therefore, H1 and H2 bind stronger than monomer which only interacts with one Protein A ligand. However, H2 binding is stronger than H1, as demonstrated by the elution order of monomer, H1 and H2 by pH gradient. This binding difference between H1 and H2 could be attributed to two factors with regard to their structure differ-

Please cite this article in press as: D. Yu, et al., Molecular perspective of antibody aggregates and their adsorption on Protein A resin, J. Chromatogr. A (2016), http://dx.doi.org/10.1016/j.chroma.2016.06.031

ence. The compact structure of H2 makes its interaction with two Protein A ligands more rigid than the flexible extended structure of H1 (Fig. 7). Furthermore, the Fab-Fab and Fc-Fc interaction of H2 exposes more of Protein A binding site between CH2 and CH3 domains for stronger Protein A interaction (Fig. S2B).

The mechanistic understanding of HMW structures and their interaction with Protein A resin provides a strong rationale to utilize Protein A chromatography for HMW removal. The stronger binding of HMWs than monomer makes it feasible to optimize the elution pH and collection signal to remove HMWs. Using this strategy, HMW removal has been achieved in Protein A step for different antibodies, which leads to improved drug substance quality. Furthermore, the HMW structures and associated charge and hydrophobicity properties could be utilized to improve polishing steps including ion exchange, hydrophobic interaction and multimodal chromatography. In addition, the potential impact of these aggregates on clinical safety and efficacy may be also derived from the structure knowledge, especially the protection and exposure of CDRs and other important surface regions.

4. Conclusions

This study discovered the structures of two distinct antibody aggregates from clarified CHO cell culture by integrating biophysical analysis and molecular modeling with process knowledge. Protein A pH gradient elution demonstrated the stronger binding of HMW than monomer and H2 than H1. The molecular weight, protein size, and Protein A binding ratio by SEC-MALS guided the structure modeling of monomer, HMW and their complex with Protein A. HDX-MS and PCA provided the molecular level interface information in H1 and H2 to support their higher order structures. Dimer H1 has an extended structure formed by Fab-Fab interaction while Dimer H2 has a compact structure formed by Fab-Fab and very likely Fc-Fc interaction. These structure difference caused stronger binding of H2 on Protein A resin than H1 although both dimers can bind two Protein A ligands. The monomer can only interact with one Protein A ligand on the resin and thus weaker binding than both dimers. The knowledge of the antibody aggregate structures and their interactions with Protein A provides mechanistic understanding for HMW removal by Protein A chromatography. The structure and properties information of aggregates and monomer could be further used to improve polishing steps and study their impact on clinical effect. The methodology of integrating biophysical analysis and molecular modeling with process development can be used for in-depth product and process understanding of biopharmaceuticals.

Conflict of interest

None.

Acknowledgments

The authors would like to acknowledge the support from Process Development Team and Process Analytical Team in Bristol-Myers Squibb Company at the Devens site. Bristol-Myers Squibb Company is acknowledged for funding support.

Appendix A. Supplementary data

Supplementary data associated with this article can be found, in the online version, at http://dx.doi.org/10.1016/j.chroma.2016.06.031.

References

[1] S. Lute, L. Norling, M. Hanson, R. Emery, D. Stinson, K. Padua, G. Blank, Q. Chen, K. Brorson, Robustness of virus removal by protein A chromatography is independent of media lifetime, J. Chromatogr. A 1205 (2008) 17–25.
[2] A.A. Shukla, P. Hinckley, Host cell protein clearance during protein A chromatography: development of an improved column wash step, Biotechnol. Progr. 24 (2008) 1115–1121.
[3] V.N. Sisodiya, J. Lequieu, M. Rodriguez, P. McDonald, K.P. Lazzareschi, Studying host cell protein interactions with monoclonal antibodies using high throughput protein A chromatography, Biotechnol. J. 7 (2012) 1233–1241.
[4] M. Vazquez-Rey, D.A. Lang, Aggregates in monoclonal antibody manufacturing processes, Biotechnol. Bioeng. 108 (2011) 1494–1508.
[5] M.E. Cromwell, E. Hilario, F. Jacobson, Protein aggregation and bioprocessing, AAPS J. 8 (2006) E572–579.
[6] A.S. Rosenberg, Effects of protein aggregates: an immunologic perspective, AAPS J. 8 (2006) E501–507.
[7] B. Sharma, Immunogenicity of therapeutic proteins. Part 3: impact of manufacturing changes, Biotechnol. Adv. 25 (2007) 325–331.
[8] R. Franco, G. Daniela, M. Fabrizio, G. Ilaria, H. Detlev, Influence of osmolarity and pH increase to achieve a reduction of monoclonal antibodies aggregates in a production process, Cytotechnology 29 (1999) 11–25.
[9] H. Pan, Methods of purifying proteins, Google Patents (2008).
[10] A. Brown, C.J. Dowd, A.N. Radhamohan, Enhanced protein purification through a modified protein a elution, Google Patents (2013).
[11] A.K. Attri, A.P. Minton, Composition gradient static light scattering: a new technique for rapid detection and quantitative characterization of reversible macromolecular hetero-associations in solution, Anal. Biochem. 346 (2005) 132–138.
[12] S.B. Geng, J.K. Cheung, C. Narasimhan, M. Shameem, P.M. Tessier, Improving monoclonal antibody selection and engineering using measurements of colloidal protein interactions, J. Pharm. Sci. 103 (2014) 3356–3363.
[13] C.A. Srebalus Barnes, A. Lim, Applications of mass spectrometry for the structural characterization of recombinant protein pharmaceuticals, Mass Spectrom. Rev. 26 (2007) 370–388.
[14] G.J. Howlett, A.P. Minton, G. Rivas, Analytical ultracentrifugation for the study of protein association and assembly, Curr. Opin. Chem. Biol. 10 (2006) 430–436.
[15] H. Nishi, M. Miyajima, N. Wakiyama, K. Kubota, J. Hasegawa, S. Uchiyama, K. Fukui, Fc domain mediated self-association of an IgG1 monoclonal antibody under a low ionic strength condition, J. Biosci. Bioeng. 112 (2011) 326–332.
[16] R.M. Ionescu, J. Vlasak, C. Price, M. Kirchmeier, Contribution of variable domains to the stability of humanized IgG1 monoclonal antibodies, J. Pharm. Sci. 97 (2008) 1414–1426.
[17] J. Guo, S. Kumar, A. Prashad, J. Starkey, S.K. Singh, Assessment of physical stability of an antibody drug conjugate by higher order structure analysis: impact of thiol- maleimide chemistry, Pharm. Res. 31 (2014) 1710–1723.
[18] J.P. Brandt, T.W. Patapoff, S.R. Aragon, Construction, MD simulation, and hydrodynamic validation of an all-atom model of a monoclonal IgG antibody, Biophys. J. 99 (2010) 905–913.
[19] L.Y. Pan, O. Salas-Solano, J.F. Valliere-Douglass, Antibody structural integrity of site-specific antibody-drug conjugates investigated by hydrogen/deuterium exchange mass spectrometry, Anal. Chem. 87 (2015) 5669–5676.
[20] R.C. Huang, G. Chen, Higher order structure characterization of protein therapeutics by hydrogen/deuterium exchange mass spectrometry, Anal. Bioanal. Chem. 406 (2014) 6541–6558.
[21] H. Wei, J. Mo, L. Tao, R.J. Russell, A.A. Tymiak, G. Chen, R.E. Iacob, J.R. Engen, Hydrogen/deuterium exchange mass spectrometry for probing higher order structure of protein therapeutics: methodology and applications, Drug Discovery Today 19 (2014) 95–102.
[22] A.J. Percy, M. Rey, K.M. Burns, D.C. Schriemer, Probing protein interactions with hydrogen/deuterium exchange and mass spectrometry—a review, Anal. Chim. Acta 721 (2012) 7–21.
[23] J.R. Engen, Analysis of protein conformation and dynamics by Hydrogen/Deuterium exchange MS, Anal. Chem. 81 (2009) 7870–7875.
[24] J. Arora, J.M. Hickey, R. Majumdar, R. Esfandiary, S.M. Bishop, H.S. Samra, C.R. Middaugh, D.D. Weis, D.B. Volkin, Hydrogen exchange mass spectrometry reveals protein interfaces and distant dynamic coupling effects during the reversible self-association of an IgG1 monoclonal antibody, MAbs 7 (2015) 525–539.
[25] X. Wang, Q. Li, M. Davies, Development of antibody arrays for monoclonal antibody Higher Order Structure analysis, Front. Pharmacol. 4 (2013) 103.
[26] S.K. Jung, K.H. Lee, J.W. Jeon, J.W. Lee, B.O. Kwon, Y.J. Kim, J.S. Bae, D.I. Kim, S.Y. Lee, S.J. Chang, Physicochemical characterization of remsima, MAbs 6 (2014) 1163–1177.
[27] R. Paul, A. Graff-Meyer, H. Stahlberg, M.E. Lauer, A.C. Rufer, H. Beck, A. Briguet, V. Schnaible, T. Buckel, S. Boeckle, Structure and function of purified monoclonal antibody dimers induced by different stress conditions, Pharm. Res. 29 (2012) 2047–2059.
[28] G. Deperalta, M. Alvarez, C. Bechtel, K. Dong, R. McDonald, V. Ling, Structural analysis of a therapeutic monoclonal antibody dimer by hydroxyl radical footprinting, MAbs 5 (2013) 86–101.
[29] A. Tramontano, The role of molecular modelling in biomedical research, FEBS Lett. 580 (2006) 2928–2934.
[30] E. Longman, K. Kreusel, S.B. Tendler, I. Fiebrig, K. King, J. Adair, P. O'Shea, A. Ortega, J. Garcia de la Torre, S.E. Harding, Estimating domain orientation of

two human antibody IgG4 chimeras by crystallohydrodynamics, Eur. Biophys. J. 32 (2003) 503–510.
[31] Y. Lu, S.E. Harding, T.E. Michaelsen, E. Longman, K.G. Davis, A. Ortega, J.G. Grossmann, I. Sandlie, J. Garcia de la Torre, Solution conformation of wild-type and mutant IgG3 and IgG4 immunoglobulins using crystallohydrodynamics: possible implications for complement activation, Biophys. J. 93 (2007) 3733–3744.
[32] N. Chennamsetty, V. Voynov, V. Kayser, B. Helk, B.L. Trout, Design of therapeutic proteins with enhanced stability, Proc. Natl. Acad. Sci. U. S. A. 106 (2009) 11937–11942.
[33] V. Kayser, N. Chennamsetty, V. Voynov, K. Forrer, B. Helk, B.L. Trout, Glycosylation influences on the aggregation propensity of therapeutic monoclonal antibodies, Biotechnol. J. 6 (2011) 38–44.
[34] L.J. Harris, S.B. Larson, K.W. Hasel, A. McPherson, Refined structure of an intact IgG2a monoclonal antibody, Biochemistry 36 (1997) 1581–1597.
[35] L.J. Harris, E. Skaletsky, A. McPherson, Crystallographic structure of an intact IgG1 monoclonal antibody, J. Mol. Biol. 275 (1998) 861–872.
[36] N. Eswar, B. Webb, M.A. Marti-Renom, M. Madhusudhan, D. Eramian, M.y. Shen, U. Pieper, A. Sali, Comparative protein structure modeling using Modeller, Curr. Protoc. Bioinf. (2006), 5.6.1–5.6.30.
[37] E.F. Pettersen, T.D. Goddard, C.C. Huang, G.S. Couch, D.M. Greenblatt, E.C. Meng, T.E. Ferrin, UCSF Chimera—a visualization system for exploratory research and analysis, J. Comput. Chem. 25 (2004) 1605–1612.
[38] H.J. Berendsen, D. van der Spoel, R. van Drunen, GROMACS: a message-passing parallel molecular dynamics implementation, Comput. Phys. Commun. 91 (1995) 43–56.
[39] M. Tashiro, R. Tejero, D.E. Zimmerman, B. Celda, B. Nilsson, G.T. Montelione, High-resolution solution NMR structure of the Z domain of staphylococcal protein A, J. Mol. Biol. 272 (1997) 573–590.
[40] E.E. Idusogie, L.G. Presta, H. Gazzano-Santoro, K. Totpal, P.Y. Wong, M. Ultsch, Y.G. Meng, M.G. Mulkerrin, Mapping of the C1q binding site on rituxan, a chimeric antibody with a human IgG1 Fc, J. Immunol. 164 (2000) 4178–4184.
[41] L. Abrahmsen, T. Moks, B. Nilsson, M. Uhlen, Construction of an igg binding protein to facilitate downstream processing using protein engineering, Google Patents (1992).
[42] H.J. Johansson, A. Ljunglof, R. Palmgren, Affinity chromatography matrix, Google Patents (2010).
[43] B. Nilsson, T. Moks, B. Jansson, L. Abrahmsen, A. Elmblad, E. Holmgren, C. Henrichson, T.A. Jones, M. Uhlen, A synthetic IgG-binding domain based on staphylococcal protein A, Protein Eng. 1 (1987) 107–113.
[44] P.-M. Åberg, GE Healthcare Bio-Sciences AB (2015).

Please cite this article in press as: D. Yu, et al., Molecular perspective of antibody aggregates and their adsorption on Protein A resin, J. Chromatogr. A (2016), http://dx.doi.org/10.1016/j.chroma.2016.06.031